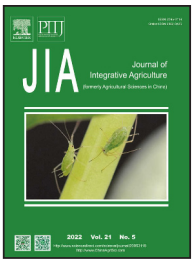
Journal of Integrative Agriculture 2022, 21(5): 1346–1356

Available online at www.sciencedirect.com

ScienceDirect



RESEARCH ARTICLE

Phenotype and mechanism analysis of plant dwarfing in pear regulated by abscisic acid

LIU Jian-long[1*], ZHANG Chen-xiao[1*], LI Tong-tong[1], LIANG Cheng-lin[2], YANG Ying-jie[1], LI Ding-Li[1], CUI Zhen-hua[1], WANG Ran[1], SONG Jian-kun[1]

[1] *College of Horticulture, Qingdao Agricultural University, Qingdao 266109, P.R.China*
[2] *Haidu College, Qingdao Agricultural University, Laiyang 265200, P.R.China*

Abstract

Close planting of dwarf varieties is currently the main cultivation direction for pear trees, and the screening of excellent dwarf varieties is an important goal for breeders. In this study, the dwarfing pear variety '601D' and its vigorous mutant '601T' were used to show their biological characteristics and further explore the dwarfing mechanism in '601D'. The biological characteristics showed that '601D' had a shorter internode length, a shorter and more compact tree body, thicker and broader leaves, lower stomata density, larger stomata size (dimension), and higher photosynthetic capacity. The biological characteristics of '601T' showed notable contrasts. The results of endogenous hormone tests indicated that the contents of abscisic acid (ABA), ABA-glucosyl ester, and GA_4 were higher in '601D', but the *trans*-zeatin content was lower. By transcriptomic analysis, significant differences were found in the biosynthetic and metabolic pathways of ABA. Related transcription factors such as bHLH, WRKY, and homeobox also participated in the regulation of plant dwarfing. We therefore examined three hormones with obvious differences with '601T', and found that only ABA could induce '601T' to return to a dwarfing plant phenotype. Therefore, we conclude that the dwarfing of '601D' is caused by an excessive accumulation of ABA. This study provides a new theoretical basis for breeding dwarf varieties.

Keywords: dwarf, pear, phenotype, abscisic acid, transcriptomic analysis

1. Introduction

Cultivation of fruit trees by the close planting of dwarf varieties has become a very important cultivation mode worldwide because of several advantages, including early fruiting, high yield, good quality, simple management, cost-effectiveness, and high profitability. At present, the main way to achieve dwarf cultivation is to use dwarfing rootstocks and dwarfing varieties. Therefore, it is of great significance to explore the dwarfing mechanisms of the dwarfing varieties. Pear is one of the most important deciduous fruit trees in the world. The total pear planting area in China has reached 937 642 ha, accounting for

Received 16 December, 2020 Accepted 11 July, 2021
Correspondence SONG Jian-kun, E-mail: qausjk@126.com; WANG Ran, E-mail: qauwr@126.com
[*] These authors contributed equally to this study.

© 2022 CAAS. Published by Elsevier B.V. This is an open access article under the CC BY-NC-ND license (http://creativecommons.org/licenses/by-nc-nd/4.0/).
doi: 10.1016/S2095-3119(21)63786-3

67.85% of the total area worldwide (http://www.fao.org/faostat/en/#data/QC) (FAQ 2018). The cultivation mode is currently changing from traditional planting to close planting of dwarf varieties, and examining the dwarfing mechanisms of the dwarfing pear trees has become a popular research topic.

To date, most dwarfing traits discovered in plants have been associated with genes involved in the biosynthesis or signaling pathways of plant hormones. Auxin is involved in the regulation of plant height. Indole-3-acetic acid (IAA), which has been recognized for more than 70 years, is essential for plant development and involved in nearly every aspect of the plant life cycle, including cell division, expansion, differentiation, lateral root formation, flowering, and trophic responses. Mutations in the GWPP (V/I) motif of Aux/IAA, which are required for auxin-induced degradation, result in auxin-related developmental defects, including short hypocotyls and stems, upwardly curled and wavy leaves, and agravitropic roots (Reed 2001; Mockaitis and Estelle 2008). In *Arabidopsis*, the gain-of-function mutant of *GH3*, which is an auxin-responsive gene, exhibits an exaggerated dwarf phenotype and resistance to exogenous auxin treatment (Nakazawa *et al.* 2001). *YABBY2b* positively regulates tomato plant height by inhibiting the expression of growth suppressor *GH3.8* (Sun *et al.* 2020). *YABBY2b* has been shown to participate in the feedback regulation of gibberellin (GA) synthesis (Liu and Li 2012; Li *et al.* 2018).

Most plant dwarf phenotypes are due to disrupted GA synthesis or signal transduction. GA has been found to regulate diverse biological processes including seed germination, stem elongation, leaf expansion, and flowering (Sun and Gubler 2004), and it is one of the most important phytohormones determining plant height (Magome *et al.* 2010). The rice semi-dwarfing mutant SD-1 exhibits GA synthesis defects and a reduced content of endogenous GA, while GA application restores plant height to the wild-type level (Sasaki *et al.* 2002). Some mutants show reduced plant height and reduced responses to GA. The mutation on the rice DELLA protein SLR1 results in dwarfing and reduced responses to GA (Ikeda *et al.* 2001).

Gibberellins are mainly synthesized by the MEP/isoprenoid pathway, and this biosynthesis can be divided into three stages (Yamaguchi and Kamiya 2000). The GA_1 and GA_2 genes play an important role in the conversion of geranylgeranyl diphosphate to ent-kaurene. The *Arabidopsis* GA_1 mutant is a GA-responsive male-sterile dwarf due to the disruption of GA biosynthesis (Yamaguchi *et al.* 1998). The phytohormones abscisic acid (ABA) and GA are well known as antagonistic partners which play an important role in controlling plant growth and development through a dynamic and complicated interaction (Zhang *et al.* 2012). ABA-inducible ATHB12, a homeodomain-leucine zipper (HD-Zip) protein of *Arabidopsis*, negatively regulates the growth of the inflorescence stem by inhibiting the expression of a gibberellin 20-oxidase gene (Son *et al.* 2010). The ABA concentration in the bark of dwarfing apple and citrus trees is higher than in vigorous varieties, and treatment with exogenous ABA has been shown to result in shortened internodes and decreased growth in two apple species (Noda *et al.* 2000; Tworkoski and Fazio 2011).

In pear, ultrastructural analysis has suggested that dwarfism is manifested by shorter and thinner stems due to a reduction in cell numbers. A higher level of endogenous ABA and higher transcript levels of the ABA pathway genes in the mutant lines revealed that the *PbPAT14* function is related to the ABA pathway (Pang *et al.* 2019). Recently, a large number of transcription factor families have been reported to be able to regulate plant dwarfing, including ARF, HD-Zip, WRKY, and NAC. Overexpression of *MdWRKY9* leads to dwarfing in apple rootstock M26 (*Malus pumila*), along with lower transcription levels of *MdDWF4* and lower levels of brassinolide (BR) (Zheng *et al.* 2018). An apple mutant with relatively short internodes and reduced cells in its stems was found to be caused by reduced levels of ABA and BR triggered by the overexpression of a novel NAC transcription factor gene *MdNAC1* (Jia *et al.* 2018). A CT repeat deletion in the promoter that causes a decrease in promoter activity is associated with lower *PcPIN-L* expression in dwarf-type pears, which might limit the polar auxin transport and in turn result in a dwarf phenotype (Zheng *et al.* 2019). MicroRNA is also involved in the regulation of pear plant height, and IAA-induced miR171f negatively regulates the IAA signaling cascade *via* the GRAS pathway to maintain apical dominance (Jiang *et al.* 2018).

Clearly, the mechanisms of plant dwarfism are very complex. In this study, we used the seeds of pear dwarf variety 'Le Nain Vert' (*Pyrus communis* L.) to breed and obtain dwarf offspring. The hybrid progeny '601D' was obtained by crossing dwarf offspring with the 'Chili' pear variety. The 610D variety has the characteristics of short trees, strong growth, late flowering, and a high affinity with pear. Therefore, '601D' is an important resource for breeding new dwarf pear varieties. The branches of dwarfing pear '601D' were treated with Co-r (60) (5 000 r min^{-1}) radiation, and one vigorous mutant was found and named '601T'. Therefore, '601D' and '601T' are ideal materials for studying the dwarfing mechanism. We used these two materials to explore the dwarfing mechanism of '601D' through morphological, histological and transcriptome

analysis. This work provides a theoretical basis for its application in production using close planting of dwarf varieties in the future.

2. Materials and methods

2.1. Plant materials

The experiment was carried out in the Jiaozhou Experiment and Demonstration Station of Qingdao Agricultural University, China (120.09°E, 36.44°N), an area with a warm temperate monsoon climate. The branches of dwarfing pear '601D' were treated with Co-r (60) (5 000 r min^{-1}) radiation and then grafted onto one-year-old rootstocks of *Pyrus betulifolia* Bunge. Among the resulting trees, one vigorous mutant was found and named '601T'. Then, '601D' and '601T' were grafted onto five-year-old rootstocks of *P. betulifolia* Bunge. Samples were collected from the shoot tips of three-year-old branches. All samples were immediately placed into liquid nitrogen and then stored at −80°C for further use.

2.2. Determination of photosynthetic indexes

The net photosynthetic rate (P_n), intercellular CO_2 (C_i), transpiration rate (T_r) and stomatal conductance (g_s) were measured using a CIRAS-3 Portable Photosynthesis System (PP Systems, USA) from 09:00 to 11:30, with the following settings: relative humidity (40±3)%, carbon dioxide concentration 390 μmol mol^{-1}, LED light source 1 200 μmol m^{-2} s^{-1}, red light 90%, and blue light 10%. The measurements were allowed to stabilize before recording. Three mature leaves from the same layer and different directions were selected from each plant for the measurements, and each treatment had ten biological replicates.

2.3. Determination of morphological structure indexes

Plant height was measured as the vertical height from the ground surface to the top of the plant. Crown breadth was measured as the south–north and east–west diameters of the pear tree. Each treatment had five biological replicates, and the average was calculated.

The annual branches of the middle-upper part were chosen for measurements of the internode length, internode diameter, shoot growth, and leaf characteristics (including leaf length, width, thickness, and area). Each treatment had 30 biological replicates.

The mature leaves on the sunny side of the same canopy were selected for measurements of the stomatal size and density. The upper epidermis of each of the harvested mature leaves was cleaned and allowed to dry naturally. The upper epidermis was peeled off and then the stomatal size was observed in 30 biological replicates under a 20× objective lens using a CX23 biomicroscope (Olympus, Japan). The number of stomata was observed under a 10× visual field, and the stomatal density was recorded as the number of stomata in each field. Ten visual fields were measured at random.

2.4. Determination of endogenous hormones

The shoot tips of three-year-old branches (50 mg fresh weight) were frozen in liquid nitrogen, ground into powder, and extracted with 1 mL methanol/water/formic acid (15:4:1, v/v). The combined extracts were evaporated to dryness under a nitrogen gas stream, reconstituted in 100 μL 80% methanol (v/v), and filtered through a 0.22-μm filter for further liquid chromatography–mass spectrometry analysis. The sample extracts were analyzed using a liquid chromatography–electrospray ionization–tandem mass spectrometry system (ExionLC Series UHPLC, Sciex, USA). The analytical conditions were as follows. High-performance liquid chromatography (HPLC) column: Waters ACQUITY UPLC HSS T3 C18 (100 mm×2.1 mm, inner diameter 1.8 μm); solvent system: water with 0.04% acetic acid (A) and acetonitrile with 0.04% acetic acid (B); gradient program: started at 5% B (0–1 min), increased to 95% B (1–8 min), held at 95% B (8–9 min), finally ramped back to 5% B (9.1–12 min); flow rate: 0.35 mL min^{-1}; temperature: 40°C; and injection volume: 2 μL. Both HPLC-grade acetonitrile and methanol were purchased from Merck (Darmstadt, Germany). MilliQ water (Millipore, Bradford, USA) was used in all experiments. All experiments were performed in triplicate using three biological replicates.

2.5. Transcriptome analysis

After RNA extraction, purification, and library establishment, the libraries were sequenced by next generation sequencing using an Illumina HiSeq Sequencing Platform. The index of the reference genome was built using HISAT2 v2.0.5, which was also used to align paired-end clean reads to the reference genome. Genes were annotated using the Dangshansuli database (http://www.ncbi.nlm.nih.gov/genome/?Term=pyrus) as a reference. Three independent biological replicates were sequenced and analyzed.

2.6. Quantification of gene expression

Total RNA was purified using an RNAprep Pure Plant Kit

(Tiangen, Beijing, China), and the RNA concentration was detected using ultraviolet spectrophotometry. Next, 1 mg of total RNA was reverse-transcribed to cDNA using a PrimeScript RT Reagent Kit with gDNA Eraser (TaKaRa, Dalian, China). Three replicates of qRT-PCR reactions were performed on a LightCycler 480 II (Roche, Basel, Switzerland) with the SYBR Premix *Ex Taq* II (TaKaRa, Dalian, China) according to the manufacturer's instructions. The primers used are listed in Appendix A.

2.7. Hormone treatment

The seedlings of '601D' and '601T' clones were selected and subcultured with Murashige and Skoog (MS) medium, The seedlings were divided into four treatments: (i) '601D' and '601T' control: continued use of the MS nutrient solution; (ii) '601T' treated with ABA: MS with 20 μmol L^{-1} ABA; (iii) '601D' treated with gibberellin (GA): MS with 40 μmol L^{-1} GA_{4+7}; and (iv) '601D' treated with isopentenyl adenosine (IPA): MS with 25 μmol L^{-1} IPA. After ABA treatment, observations were carried out after 20 days, while observations of the GA and IPA treatments were postponed to 30 days.

2.8. Statistical analysis

Treatment differences were tested using Student's *t*-test at $P<0.05$ in SPSS 23.0. Results are presented as mean±standard deviation (SD) of at least three replicate samples.

3. Results

3.1. Comparison of '601D' and '601T' phenotypes

The phenotypic difference between '601D' and '601T' was obvious. The '601D' tree was short and compact, while '601T' was tall with large divergent branches. The plant height and crown breadth of '601T' were much larger than those of '601D', and these differences were significant (Fig. 1-A; Table 1). The results showed that the branches of '601D' were thicker than those of '601T' (Fig. 1-B). The internode length of the '601T' branches was significantly greater than that of '601D', reaching 31.05 mm, while the branch diameter was significantly smaller than that of '601D' (only 2.95 mm) (Table 1).

3.2. Comparison of photosynthetic characteristics between '601D' and '601T'

The net photosynthetic rate of '601D' was 19.36 μmol m^{-2} s^{-1}, which was higher than that of '601T' (9.78 μmol m^{-2} s^{-1}). The intercellular CO_2 concentration (C_i), transpiration rate (T_r), and stomatal conductance (g_s) of '601D' were significantly higher than those of '601T' (Fig. 2). The leaves of '601D' were larger and thicker, while those of '601T' were relatively smaller and thinner. The leaf thickness, leaf area, leaf length, leaf width, petiole length, and petiole diameter of '601T' were significantly lower than those of '601D'. The leaf area of dwarfing '601D' was 3 636.70 mm^2, while that of vigorous mutant '601T' was 1 636.7 mm^2 (Fig. 1-C; Table 1).

Under the light microscope, differences in the leaf

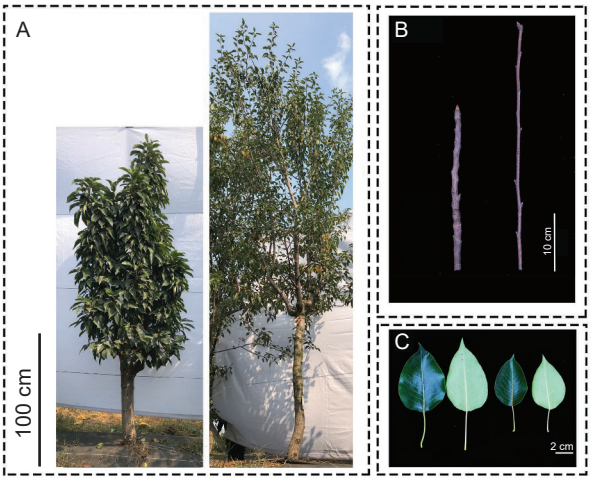


Fig. 1 Morphological characteristics of '601D' and '601T'. A, tree structure. B, branch morphology. C, leaf morphology.

Table 1 Comparison of morphological leaf indexes of '601D' and '601T'

Strain	Leaf thickness (mm)	Leaf area (mm^2)	Leaf length (mm)	Leaf width (mm)
601D	0.37±0.06 a	3 636.70±134.50 a	106.22±12.14 a	58.48±5.02 a
601T	0.26±0.01 b	1 636.7±90.50 b	67.13±1.38 b	38.66±0.30 b
Strain	Plant height (cm)	Crown width (cm)	Internode length (mm)	Internode roughness (mm)
601D	245±18.37 b	71±2.45 b	10.01±0.59 b	6.28±0.27 a
601T	452±17.72 a	236±16.39 a	31.05±1.45 a	2.95±0.09 b

Values are mean±SD of at least five replicates. Different letters within a column indicate significant differences using Student's *t*-test ($P<0.05$).

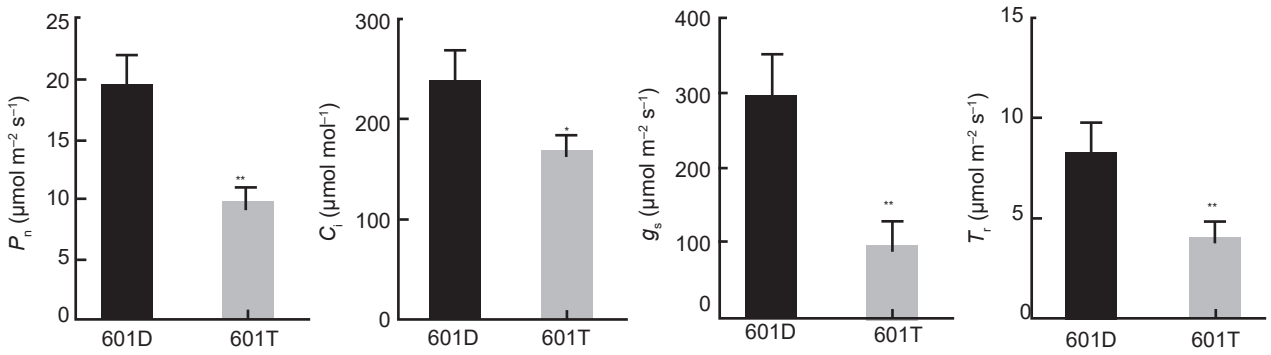


Fig. 2 Comparison of photosynthesis characteristics between '601D' and '601T'. P_n, net photosynthetic rate; C_i, intercellular CO_2 concentration; g_s, stomatal conductance; and T_r, transpiration rate. Values are mean±SD of ten replicates. Asterisks indicate significance using Student's *t*-test (*, $P<0.05$; **, $P<0.01$).

stomata were found between '601D' and '601T'. The stomatal transverse diameter (23.71 μm) and vertical diameter (36.10 μm) of '601D' were significantly larger than those of '601T', but the stomatal density of '601D' was lower than that of '601T', and these differences were significant (Fig. 3; Table 2).

3.3. Determination of endogenous hormones

The endogenous hormone contents in the shoot tips of '601D' and '601T' were determined. The results showed that there were no significant differences in the IAA or IPA contents between '601D' and '601T'. However, the ABA and ABA-glucosyl ester (ABA-GE) contents in '601D' were significantly higher than those in '601T'. The *trans*-zeatin content in '601T' was significantly higher than in '601D', while there was no significant difference in the content of *cis*-zeatin. In '601D', the GA_4 content was significantly higher than that in '601T', but there was no significant difference in GA_1 (Fig. 4).

3.4. Transcriptome analysis

After removing low-quality reads from the transcriptome data, the reads were compared with the reference genome database of *Pyrus×bretschneideri*, and the reads from the comparison were then classified and annotated. The mapping efficiency of reads and the *Pyrus×bretschneideri* reference genome of all samples was above 71%, meeting the needs of subsequent analysis (Table 3). There were 489 differentially expressed genes in the differential transcriptome of '601D' and '601T', of which 414 genes were up-regulated and 75 genes were down-regulated (Appendix B). Among these, 41 hormone-related genes were screened, involving auxin, abscisic acid, ethylene, cytokinin, gibberellin, and so on; 67 transcription factors were also screened, including bHLH, WRKY, MYB, TCP, LDSH, ERF, homeobox, and other transcription factor families (Fig. 5; Appendix B).

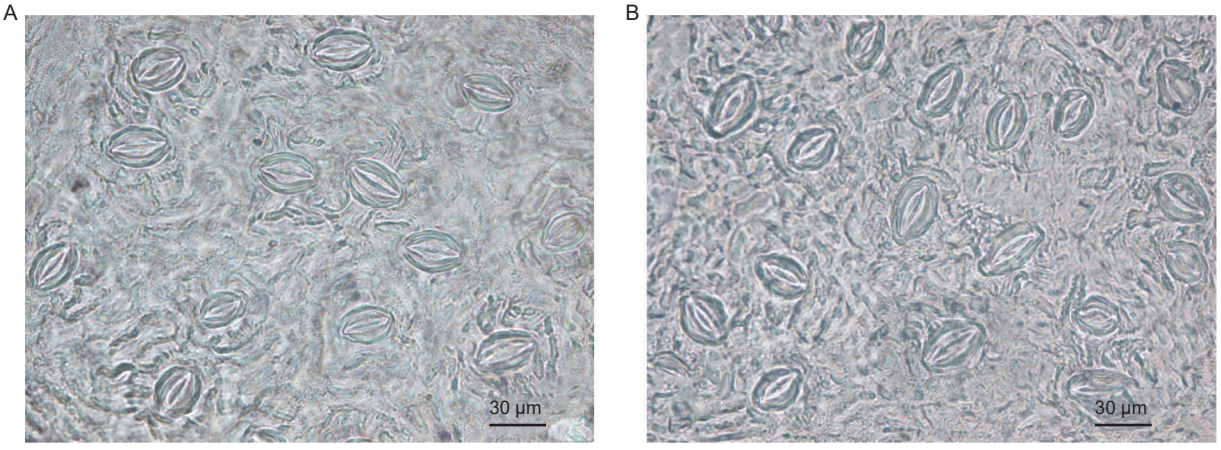


Fig. 3 Comparison of stomatal morphology between '601D' (A) and '601T' (B).

Table 2 Comparison of stomatal morphology between '601D' and '601T' leaves

Strain	Number per view	Transverse diameter (μm)	Vertical diameter (μm)
601D	39.1±0.59 b	23.71±0.69 a	36.10±1.68 a
601T	46.5±2.13 a	21.34±0.42 b	32.17±0.71 b

Values are mean±SD of ten replicates. Different letters within a column indicate significant differences using Student's *t*-test (P<0.05).

Furthermore, six genes were randomly selected, and their expression levels were verified to be consistent with those in the transcriptome (Fig. 6).

3.5. Responses of '601D' and '601T' plants to hormones

The explants of '601D' and '601T' were treated with different hormones, and the dwarf phenotype of '601T' plants was restored at 20 days after ABA treatment. However, '601D' treated with GA_{4+7} or IPA did not show the slender phenotype (Fig. 7).

4. Discussion

The current trend in global pear fruit production is to cultivate grafted trees in modern orchards by grafting pear cultivar scions onto dwarfing rootstocks (Qi *et al.* 2020). As dwarfing rootstocks simplify orchard management and reduce production costs, there is great interest in producing superior dwarfing rootstocks for pear and understanding the basic mechanism of plant dwarfism (Prassinos *et al.* 2009; Ou *et al.* 2015).

In our study, '601T' was mutated by radiation. As a vigorous mutant, the '601T' trees were tall. The tree height and crown breadth were both greater than those of '601D'. The characteristics of '601T' branches were obvious, with slender branches and longer internodes, which showed significant differences from '601D'. Although '601D' is a dwarfing variety, it grows vigorously. Meanwhile, '601D' also had a stronger photosynthetic capacity. The net photosynthetic rate of '601D' was significantly higher than that of '601T', and the transpiration was stronger. The g_s and C_i values of '601D' were both higher than those of '601T'. The '601D' tree was more robust and had wider leaves, and its leaf area and leaf thickness were much greater than those of '601T'. Numerous studies have reported a direct positive relationship between dry-matter content improvements and increases in the net photosynthetic rate (Murchie *et al.* 2018; Sanchez-Bragado *et al.* 2020). This may be

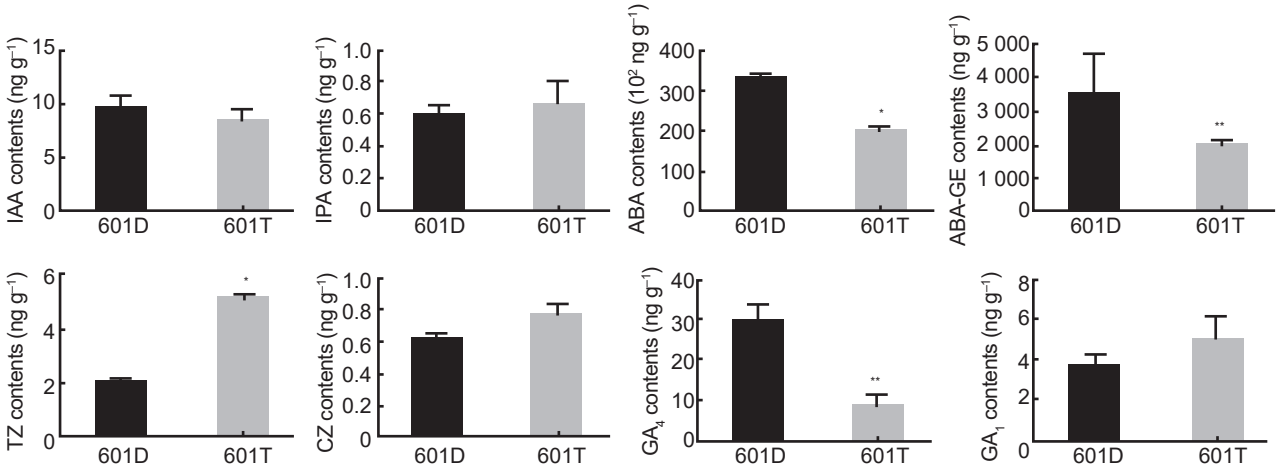


Fig. 4 Comparison of endogenous hormone contents between '601D' and '601T'. IAA, indole-3-acetic acid; IPA, isopentenyl adenosine; ABA, abscisic acid; ABA-GE, ABA-glucosyl ester; TZ, *trans*-zeatin; CZ, *cis*-zeatin; GA_4, gibberellin 4; GA_1, gibberellin 1. Values are mean±SD of three replicates. Asterisks indicate significance using Student's *t*-test (*, P<0.05; **, P<0.01).

Table 3 List of mapping results

Sample	Clean reads	Total mapped	Multiple mapped	Uniquely mapped
601D1	39 581 128	28 129 228 (71.07%)	2 934 424 (10.43%)	25 194 804 (89.57%)
601D2	43 595 990	31 311 025 (71.82%)	3 281 079 (10.48%)	28 029 946 (89.52%)
601D3	40 796 800	29 159 060 (71.47%)	3 144 337 (10.78%)	26 014 723 (89.22%)
601T1	44 517 446	31 879 649 (71.61%)	3 374 997 (10.59%)	28 504 652 (89.41%)
601T2	41 877 950	30 192 791 (72.10%)	3 168 980 (10.50%)	27 023 811 (89.50%)
601T3	43 521 972	31 273 531 (71.86%)	3 303 951 (10.56%)	27 969 580 (89.44%)

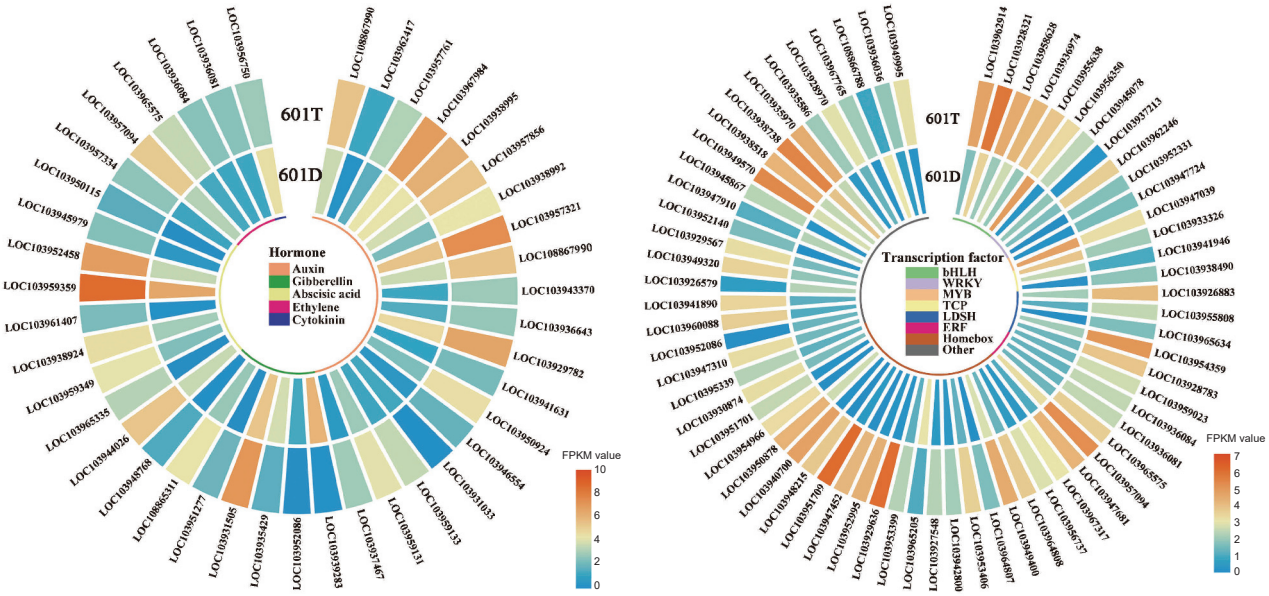


Fig. 5 Relative expression levels of auxin, gibberellin, abscisic acid, ethylene, cytokinin, and transcription factor-related genes. A, hormone-related genes. B, transcription factor-related genes.

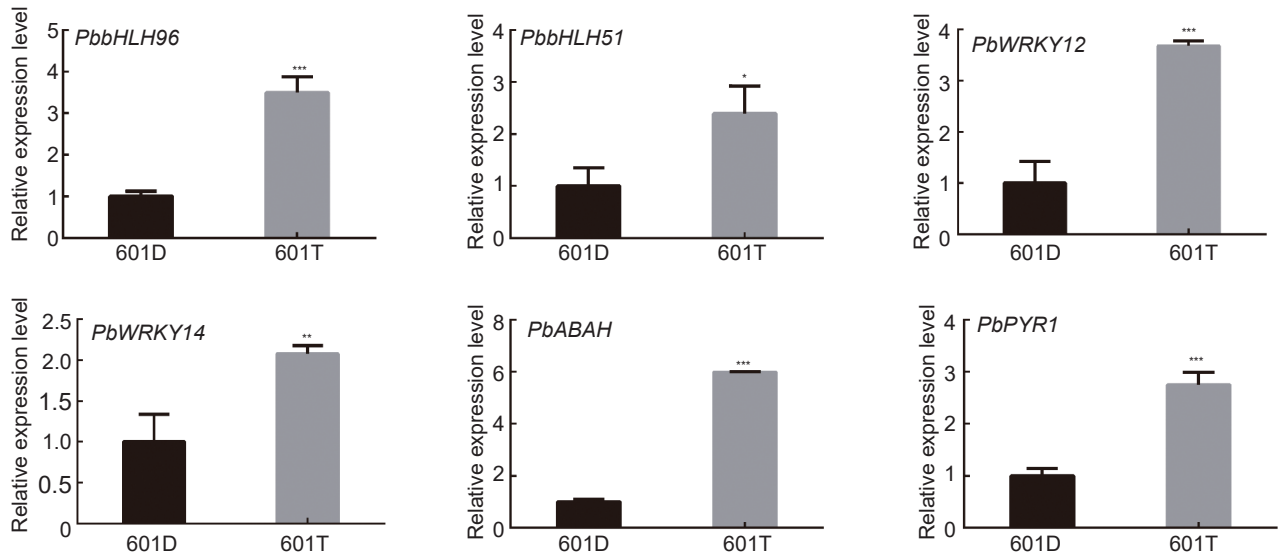


Fig. 6 Relative expression levels of transcription factor- and abscisic acid-related genes between '601D' and '601T'. Values are mean±SD of three replicates. Asterisks indicate significance using Student's *t*-test (*, $P<0.05$; **, $P<0.01$; ***, $P<0.001$).

the main reason for the vigorous growth of '601D'. It is therefore of practical significance to study the dwarfing mechanism of '601D'.

By stomatal observation, it was found that the stomatal density of '601D' was smaller than that of '601T', but the stomatal size was significantly greater than that of '601T'. It is well known that stomatal closure in plants is regulated by ABA (Guo *et al*. 2020; Zhao *et al*. 2020). In our study, the ABA content of '601D' was significantly higher than that of '601T'. It has been shown that ABA can be reversibly inactivated by glucosylation, while ABA-GE is an inactive storage and transfer form (Schroeder and Nambara 2006). The content of ABA-GE in '601D' was significantly higher than in '601T', which indicated that the total amount of ABA in '601D' was higher than in '601T', and ABA accumulated in '601D'. It has been shown that ABA can inhibit plant growth and cause a dwarfing phenotype (Han *et al*. 2012; Fu *et al*. 2014). Furthermore,

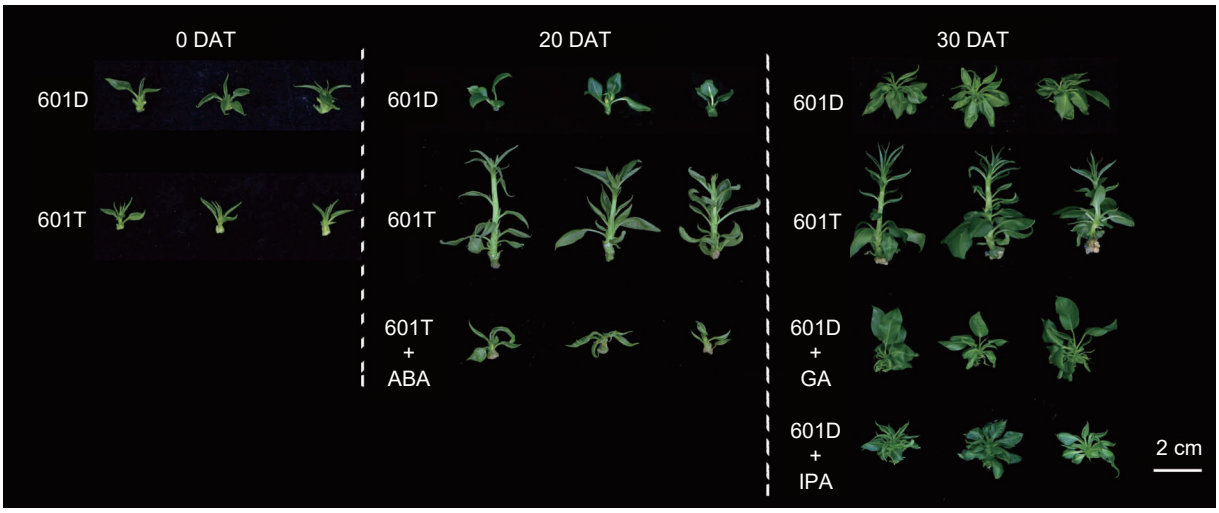


Fig. 7 Morphological comparisons of '601D' and '601T' treated with different hormones. ABA, treated with 20 μmol L^{-1} abscisic acid (ABA); GA, treated with 40 μmol L^{-1} gibberellin 4+7 (GA_{4+7}); IPA, treated with 25 μmol L^{-1} isopentenyl adenosine (IPA). DAT, days after treatment.

we found that the key genes for 9-*cis*-epoxycarotenoid dioxygenase (NCED) and ABAH in the ABA synthesis pathway were significantly different between the two varieties. NCED is known to be a key enzyme in the ABA synthesis pathway and can regulate ABA accumulation. However, it has been reported that NCED can reduce ABA content with its increased expression (Audran *et al.* 1998). Furthermore, ABAH is a key rate-limiting enzyme in the ABA synthesis pathway, and its expression is negatively correlated with ABA (Ji *et al.* 2018). This is consistent with our finding that ABAH was significantly up-regulated in '601T'. Generally, the g_s of plants decreased when ABA content was increased (Pantin *et al.* 2013). There are two main reasons for this result. One is that the sampling position is different. For hormone determination, the shoot tip tissue is the material, and the photosynthetic index is determined by using the leaf. Although '601D' is dwarf, its leaves grow vigorously, and their thickness and size are greater than in '601T', which may be the reason for its higher photosynthetic capacity.

We know that gibberellin and cytokinin mainly promote cell elongation and division. Gibberellins were first identified as fungal compounds that promote stem elongation. Later, gibberellins were further shown to promote stem elongation and seed germination (Lester *et al.*1997), while increasing cytokinin levels were also found to enhance shoot growth (Kurakawa *et al.* 2007; Kuroha *et al.* 2009). Interestingly, the content of GA_4 in '601D' was higher than in '601T'. Although the high-activity *trans*-zeatin in '601D' was lower than in '601T', exogenous GA and cytokinin could not promote plant height. Therefore, this was not the cause of dwarfing, but it was probably the main reason for leaf enlargement and plant growth.

To analyze the dwarfing mechanism of the two varieties from the perspective of expression regulation, we screened 489 differentially expressed genes. Among them, 414 genes were up-regulated and 75 genes were down-regulated in '601T', including 67 transcription factors that mainly belong to the bHLH, homeobox, and WRKY families. These families of genes play an important role in plant dwarfing. For example, overexpression of *CubHLH1* was found to be the cause of a dwarf phenotype in transgenic tomato (*Solanum lycopersicum* L.), and the abscisic acid contents of all the transgenic tomato fruit were found to be higher than that of the wild type (Endo *et al.* 2016). KNOX1, a member of the homeobox family, is induced by ABA and acts on the downstream of ABA. The high expression of STM could inhibit the decrease in lignin content, and the mutant plants showed a short-stem phenotype (Lee *et al.* 2016; Xie *et al.* 2017). Small grain, semi-dwarf 3 and WRKY71 negatively regulate plant height and grain size by stabilizing SLR1 expression in rice (Guo *et al.* 2015; Lan *et al.* 2020). These transcription factors may be involved in the regulation of plant dwarfism, but this needs further study.

In addition, we found that seven members of the P450 gene family were differentially expressed, and six of them were up-regulated. Previous studies have shown that P450 reduces the amount of ABA flowing in the vascular tissue, while CYP707A1 inactivates the local ABA pool in guard cells (Okamoto *et al.* 2009). While P450 inhibitors are non-specific, uniconazole inhibits ABA inactivation and

GA synthesis, causing growth reduction (Kitahata *et al.* 2005; Todoroki *et al.* 2008). Therefore, P450 may act on the upstream of ABA to regulate ABA synthesis. When '601T' explants were treated with ABA, we found that the dwarfing phenotype was restored after 20 days of growth, which indicated that the dwarfing of '601D' was caused by the accumulation of ABA. However, when '601D' was treated with gibberellin and cytokinin, it did not increase in height. The content of GA_4 in '601D' was higher than in '601T', which may be the reason why the growth of '601D' was not inhibited even though it was dwarfed.

5. Conclusion

The mechanism of the dwarfism of '601D' was analyzed from the perspectives of phenotypic observations and transcriptional regulation by comparison with '601T'. We found that in '601D', the internodes were shorter, the leaves were thicker and the photosynthetic capacity was higher. Gibberellin and cytokinin increased in '601D', but this did not increase its height. The '601T' explants were dwarfed after ABA treatment. The analysis of transcriptional regulation showed that the ABA hormones and related regulatory pathways in '601T' and '601D' were regulated. The transcription levels of the WRKY, homeobox, and bHLH family were significantly different, and their functions will be studied further in future work.

Acknowledgements

This research was funded by the National Key Research and Development Program of China (2018YFD1000100), the Agricultural Improved Variety Project Program of Shandong Province, China (2019LZGC008), and the National Key Research and Development Program of China (2019YFD1001404-3).

Declaration of competing interest

The authors declare that they have no conflict of interest.

Appendices associated with this paper are available on http://www.ChinaAgriSci.com/V2/En/appendix.htm

References

Audran C, Borel C, Fre A, Sotta B, Meyer C, Simonneau T, Marion-Poll A. 1998. Expression studies of the zeaxanthin epoxidase gene in *Nicotiana plumbaginifolia*. *Plant Physiology*, **118**, 1021–1028.

Endo T, Fujii H, Sugiyama A, Nakano M, Nakajima N, Ikoma Y, Omura M, Shimada T. 2016. Overexpression of a citrus basic helix-loop-helix transcription factor (*CubHLH1*), which is homologous to *Arabidopsis* activation-tagged bri1 suppressor 1 interacting factor genes, modulates carotenoid metabolism in transgenic tomato. *Plant Science*, **243**, 35–48.

FAO (Food and Agriculture Organization of the United Nations). 2018. FAOSTAT, FAO statistical databases. [2018-11-21]. http://www.fao.org/faostat/en/#data/QC

Fu M, Kang H K, Son S H, Kim S K, Nam K H. 2014. A subset of *Arabidopsis* RAV transcription factors modulates drought and salt stress responses independent of ABA. *Plant and Cell Physiology*, **55**, 1892–1904.

Guo D S, Zhang J Z, Wang X L, Han X, Wei B Y, Wang J Q, Li B X, Yu H, Huang Q P, Gu H Y, Qu L J, Qin G J. 2015. The WRKY transcription factor WRKY71/EXB1 controls shoot branching by transcriptionally regulating *RAX* genes in *Arabidopsis*. *Plant Cell*, **27**, 3112–3127.

Guo Z L, Xu H N, Lei Q D, Du J C, Li C, Wang C D, Yang Y Q, Yang Y P, Sun X D. 2020. The *Arabidopsis* transcription factor LBD15 mediates ABA signaling and tolerance of water-deficit stress by regulating *ABI4* expression. *Plant Journal*, **104**, 510–521.

Han Y J, Cho K C, Hwang O J, Choi Y S, Shin A Y, Hwang I, Kim J I. 2012. Overexpression of an *Arabidopsis* β-glucosidase gene enhances drought resistance with dwarf phenotype in creeping bentgrass. *Plant Cell Reports*, **31**, 1677–1686.

Ikeda A, Ueguchi-Tanaka M Y, Kitano H, Koshioka M, Futsuhara Y. 2001. Slender rice, a constitutive gibberellin response mutant, is caused by a null mutation of the *SLR1* gene, an ortholog of the height-regulating gene *GAI/RGA/RHT/D8*. *Plant Cell Environment*, **13**, 999–1010.

Ji J, Yue J Y, Xie T T, Chen W, Du C J, Chang E M, Chen L Z, Jiang Z P, Shi S Q. 2018. Roles of γ-aminobutyric acid on salinity-responsive genes at transcriptomic level in poplar: Involving in abscisic acid and ethylene-signalling pathways. *Planta*, **248**, 675–690.

Jia D, Gong X, Li M, Li C, Sun T, Ma F. 2018. Overexpression of a novel apple NAC transcription factor gene, *MdNAC1*, confers the dwarf phenotype in transgenic apple (*Malus domestica*). *Genes*, **5**, 229.

Jiang S L, Chen Q J, Zhang Q L, Zhang Y, Hao N N, Ou C Q, Wang F, Li T Z. 2018. Pyr-miR171f-targeted *PyrSCL6* and *PyrSCL22* genes regulate shoot growth by responding to IAA signaling in pear. *Tree Genetics & Genomes*, **14**, 20.

Kitahata N, Saito S, Miyazawa Y, Umezawa T, Shimada Y, Min Y K, Mizutani M, Hirai N, Shinozaki K, Yoshida S, Asami T. 2005. Chemical regulation of abscisic acid catabolism in plants by cytochrome P450 inhibitors. *Bioorganic & Medicinal Chemistry*, **13**, 4491–4498.

Kurakawa T, Ueda N, Maekawa M, Kobayashi K, Kojima M, Nagato Y, Sakakibara H, Kyozuka J. 2007. Direct control of shoot meristem activity by a cytokinin-activating enzyme. *Nature*, **445**, 652–655.

Kuroha T, Tokunaga H, Kojima M, Ueda N, Ishida T, Nagawa S, Fukuda H, Sugimoto K, Sakakibara H. 2009. Functional analyses of *LONELY GUY* cytokinin-activating enzymes reveal the importance of the direct activation pathway in

Arabidopsis. *Plant Cell*, **21**, 3152–3169.

Lan J, Lin Q B, Zhou C L, Ren Y K, Liu X, Miao R, Jing R N, Mou C L, Nguyen T, Zhu X J, Wang Q, Zhang, X, Guo X P, Liu S J, Jiang L, Wan J M. 2020. Small grain and semi-dwarf 3, a *WRKY* transcription factor, negatively regulates plant height and grain size by stabilizing *SLR1* expression in rice. *Plant Molecular Biology*, **104**, 429–450.

Lee H G, Choi Y R, Seo P J. 2016. Increased *STM* expression is associated with drought tolerance in *Arabidopsis*. *Journal of Plant Physiology*, **201**, 79–84.

Lester D R, Ross J J, Davies P J, Reid J B. 1997. Mendel's stem length gene (*Le*) encodes a gibberellin 3β-hydroxylase. *Plant Cell*, **9**, 1435–1443.

Li H, Sun M, Qi M, Xing J, Xu T, Liu H, Li T. 2018. Alteration of *SlYABBY2b* gene expression impairs tomato ovary locule number and endogenous gibberellin content. *Journal of Zhejiang University* (Science B), **18**, 445–457.

Liu S, Li T L. 2012. Regulation effects of exogenous gibberellin acid (GA_3) on the formation of tomato (*Solanum Lycoperscium*) ovary locule and fasciated transcription. *African Journal of Biotechnology*, **11**, 13732–13738.

Magome H, Yamaguchi S, Hanada A, Kamiya Y, Oda K. 2010. Dwarf and delayed-flowering 1, a novel *Arabidopsis* mutant deficient in gibberellin biosynthesis because of overexpression of a putative *AP2* transcription factor. *Plant Journal*, **37**, 720–729.

Mockaitis K, Estelle M. 2008. Auxin receptors and plant development: A new signaling paradigm. *Annual Review of Cell and Developmental Biology*, **24**, 55–80.

Murchie E H, Kefauver S, Araus J, Muller O, Rascher U, Flood P J, Lawson T. 2018. Measuring the dynamic photosynthome. *Annals of Botany*, **122**, 207–220.

Nakazawa M, Yabe N, Ichikawa T, Yamamoto Y Y, Yoshizumi T, Hasunuma K, Matsui M. 2001. *DFL1*, an auxin-responsive *GH3* gene homologue, negatively regulates shoot cell elongation and lateral root formation, and positively regulates the light response of hypocotyl length. *Plant Journal*, **25**, 213–221.

Noda K, Okuda H, Iwagaki I. 2000. Indole acetic acid and abscisic acid levels in new shoots and fibrous roots of citrus scion-rootstock combinations. *Scientia Horticulturae*, **84**, 245–254.

Okamoto M, Tanaka Y, Abrams S R, Kamiya Y, Seki M, Nambara E. 2009. High humidity induces abscisic acid 8′-hydroxylase in stomata and vasculature to regulate local and systemic abscisic acid responses in *Arabidopsis*. *Plant Physiology*, **149**, 825–834.

Ou C, Jiang S, Wang F, Tang C, Hao N. 2015. An RNA-Seq analysis of the pear (*Pyrus communis* L.) transcriptome, with a focus on genes associated with dwarf. *Plant Gene*, **4**, 69–77.

Pang H G, Yan Q, Zhao S L, He F, Xu J F, Qi B X, Zhang Y X. 2019. Knockout of the S-acyltransferase gene, *PbPAT14*, confers the dwarf yellowing phenotype in first-generation pear by ABA accumulation. *International Journal of Molecular Sciences*, **20**, 6347.

Pantin F, Monnet F, Jannaud D, Costa J M, Renaud J, Muller B, Simonneau T, Genty B. 2013. The dual effect of abscisic acid on stomata. *New Phytologist*, **197**, 65–72

Prassinos C, Ko J H, Lang G, Iezzoni A F, Han K H. 2009. Rootstock-induced dwarfing in cherries is caused by differential cessation of terminal meristem growth and is triggered by rootstock-specific gene regulation. *Tree Physiology*, **29**, 927–936.

Qi L Y, Chen L, Wang C S, Zhang S L, Yang Y J, Liu J L, Li D L, Song J K, Wang R. 2020. Characterization of the auxin efflux transporter PIN proteins in pear. *Plants*, **9**, 349.

Reed W J. 2001. Roles and activities of Aux/IAA proteins in *Arabidopsis*. *Trends in Plant Science*, **6**, 420–425.

Sanchez-Bragado R, Vicente R, Molero G, Serret M D, Maydupe M L, Araus J L. 2020. New avenues for increasing yield and stability in C3 cereals: Exploring ear photosynthesis. *Current Opinion in Plant Biology*, **56**, 223–234.

Sasaki A, Ashikari M, Ueguchi-Tanaka M, Itoh H, Nishimura A, Swapan D, Ishiyama K, Saito T, Kobayashi M, Khush G S, Kitano H, Matsuoka M. 2002. A mutant gibberellin-synthesis gene in rice. *Nature*, **416**, 701–702.

Schroeder J I, Nambara E. 2006. A quick release mechanism for abscisic acid. *Cell*, **126**, 1023–1025.

Son O, Hur Y S, Kim Y K, Lee H J, Kim S, Kim M R, Nam K H, Lee M S, Kim B Y, Park J, Lee S C, Hanada A, Yamaguchi S, Lee I J, Kim S K, Yun D J, Soderman E, Cheon C I. 2010. *ATHB12*, an ABA-inducible homeodomain-leucine zipper (*HD-Zip*) protein of *Arabidopsis*, negatively regulates the growth of the inflorescence stem by decreasing the expression of a gibberellin 20-oxidase gene. *Plant and Cell Physiology*, **51**, 1537–1547.

Sun M H, Li H, Li Y B, Xiang H Z, Liu Y D, He Y, Qi M F, Li T L. 2020. Tomato *YABBY2b* controls plant height through regulating *indole-3-acetic acid-amido synthetase* (*GH3.8*) expression. *Plant Science*, **297**, 110530.

Sun T, Gubler F. 2004. Molecular mechanism of gibberellin signaling in plants. *Annual Review of Plant Biology*, **55**, 197–223.

Todoroki Y, Kobayashi K, Yoneyama H, Hiramatsu S, Jin M H, Watanabe B, Mizutani M, Hirai N. 2008. Structure–activity relationship of uniconazole, a potent inhibitor of ABA 8′-hydroxylase, with a focus on hydrophilic functional groups and conformation. *Bioorganic & Medicinal Chemistry*, **16**, 3141–3152.

Tworkoski T, Fazio G. 2011. Physiological and morphological effects of size-controlling rootstocks on 'Fuji' apple scions. *Acta Horticulturae*, **903**, 865–872.

Xie C M, Zhang G, Zhang Y M, Song X G, Guo H Y, Chen X Y, Fang R X. 2017. *SRWD1*, a novel target gene of DELLA and WRKY proteins, participates in the development and immune response of rice (*Oryza sativa* L.). *Science Bulletin*, **62**, 1639–1648.

Yamaguchi S, Kamiya Y. 2000. Gibberellin biosynthesis: Its regulation by endogenous and environmental signals. *Plant and Cell Physiology*, **41**, 251–257.

Yamaguchi S, Sun T, Kawaide H, Kamiya Y. 1998. The GA_2 locus of *Arabidopsis thaliana* encodes *ent*-kaurene synthase of gibberellin biosynthesis. *Plant Physiology*, **116**, 1271–1278.

Zhang Y, Feng F, He C Z. 2012. Downregulation of *OsPK1* contributes to oxidative stress and the variations in ABA/GA balance in rice. *Plant Molecular Biology Reporter*, **30**, 1006–1013.

Zhao S, Gao H B, Jia X M, Wang H B, Ke M, Ma F W. 2020. The HD-Zip I transcription factor *MdHB-7* regulates drought tolerance in transgenic apple (*Malus domestica*). *Environmental and Experimental Botany*, **180**, 104246.

Zheng X, Zhao Y, Shan D, Shi K, Wang L, Li Q, Wang N, Zhou J, Yao J, Xue Y, Fang S, Chu J, Guo Y, Kong J. 2018. *MdWRKY9* overexpression confers intensive dwarfing in the M26 rootstock of apple by directly inhibiting brassinosteroid synthetase *MdDWF4* expression. *New Phytologist*, **217**, 1086–1098.

Zheng X D, Zhang H Y, Xiao Y X, Wang C H, Tian Y K. 2019. Deletion in the promoter of *PcPIN-L* affects the polar auxin transport in dwarf pear (*Pyrus communis* L.). *Scientific Reports*, **9**, 18645.

Executive Editor-in-Chief HUANG San-wen
Managing Editor WENG Ling-yun